

Tunable dual-core liquid-filled photonic crystal fibers for dispersion compensation

Chin-ping Yu^{1*}, Jia-hong Liou¹, Sheng-shuo Huang¹, and Hung-chun Chang²

¹*Institute of Electro-Optical Engineering and Advanced Crystal Opto-electronic Research Center
National Sun Yat-Sen University, Kaohsiung, Taiwan 80424, R. O. C.*

²*Graduate Institute of Photonics and Optoelectronics, Graduate Institute of Communication Engineering, and
Department of Electrical Engineering, National Taiwan University, Taipei, Taiwan 10617, R. O. C.
cpyu@faculty.nsysu.edu.tw*

Abstract: We have theoretically investigated the dispersion characteristics of dispersion compensating fibers based on dual-core liquid-filled PCFs. A very high negative chromatic dispersion value $D = -19000$ ps/(nm-km) can be achieved at 1.55- μm wavelength by an appropriate design. By varying the geometry of the PCF and the index of the filling liquid, the phase-matching wavelength and dispersion values are shown to be well tuned to desired values. The proposed structure also demonstrates good tunable properties with operation temperature for optical communication systems.

©2008 Optical Society of America

OCIS codes: (060.2280) Fiber design and fabrication; (060.5295) Photonic crystal fiber

References and links

1. D. Garthe, R. E. Epworth, W. S. Lee, A. Hadjifotiou, C. P. Chew, T. Bricheno, A. Fielding, H. N. Rourke, S. R. Barker, K. C. Byron, R. S. Baulcomb, S. M. Ohja, and D. Clements, "Adjustable dispersion equalizer for 10 and 20 Gbit/s over distances up to 160km," *Electron. Lett.* **30**, 2159–2160 (1994).
2. B. J. Eggleton, K. A. Ahmed, F. Ouellette, P. A. Krug, and H.-F. Liu, "Recompression of pulses broadened by transmission through 10 km of non-dispersion-shifted fiber at 1.55 μm using 40-mm-long optical fiber Bragg gratings with tunable chirp and central wavelength," *IEEE Photon. Technol. Lett.* **7**, 494–496 (1995).
3. K. Takiguchi, K. Okamoto, and K. Moriwaki, "Planar lightwave circuit dispersion equalizer," *J. Lightwave Technol.* **14**, 2003–2011 (1996).
4. C. D. Poole, J. M. Weisenfeld, and D. J. Giovanni, "Elliptical-core dual-mode fiber dispersion compensator," *IEEE Photon. Technol. Lett.* **5**, 194–197 (1993).
5. A. H. Gnauck, L. D. Garrett, Y. Danziger, U. Levy, and M. Tur, "Dispersion and dispersion-slope compensation of NZDSF over the entire C band using higher-order-mode fibre," *Electron. Lett.* **36**, 1946–1947 (2000).
6. K. Thyagarajan, R. K. Varshney, P. Palai, A. K. Ghatak, and I. C. Goyal, "A novel design of a dispersion compensating fiber," *IEEE Photon. Technol. Lett.* **8**, 1510–1512 (1996).
7. J.-L. Auguste, R. Jindal, J.-M. Blondy, M. Clapeau, J. Marcou, B. Dussardier, G. Monnom, D. B. Ostrowsky, B. P. Pal, and K. Thyagarajan, "-1800 ps/(nm.km) chromatic dispersion at 1.55 μm in dual concentric core fibre," *Electron. Lett.* **36**, 1689–1691 (2000).
8. L. Gröner-Nielsen, S. N. Knudsen, B. Edvold, T. Veng, D. Magnussen, C. C. Larsen, and H. Damsgaard, "Dispersion compensating fibers," *Opt. Fiber Technol.* **6**, 164–180 (2000).
9. K. Pande and B. P. Pal, "Design optimization of a dual-core dispersion-compensating fiber with a high figure of merit and a large effective area for dense wavelength-division multiplexed transmission through standard G.655 fibers," *Appl. Opt.* **42**, 3785–3791 (2003).
10. J. Broeng, D. Mogilevstev, S. E. Barkou, and A. Bjarklev, "Photonic crystal fibers: A new class of optical waveguides," *Opt. Fiber Technol.* **5**, 305–330, (1999).
11. C. P. Yu and H. C. Chang, "Applications of the finite difference mode solution method to photonic crystal structures," *Opt. Quantum Electron.* **36**, 145–163 (2004).
12. L. P. Shen, W.-P. Huang, G. X. Chen, and S. S. Jian, "Design and optimization of photonic crystal fibers for broad-band dispersion compensation," *IEEE Photon. Technol. Lett.* **15**, 540–542 (2003).
13. F. Poli, A. Cucinotta, M. Fucchi, S. Selleri, and L. Vincetti, "Characterization of microstructured optical fibers for wideband dispersion compensation," *J. Opt. Soc. Am. A* **20**, 1958–1962 (2003).
14. L. P. Shen, W.-P. Huang, and S. S. Jian, "Design of photonic crystal fibers for dispersion-related applications," *J. Lightwave Technol.* **21**, 1644–1651 (2003).
15. B. Zsigri, J. Laegsgaard, and A. Bjarklev, "A novel photonic crystal fibre design for dispersion compensation," *J. Opt. A: Pure Appl. Opt.* **6**, 717–720 (2004).

16. Y. Ni, L. An, J. Peng, and C. Fan, "Dual-core photonic crystal fiber for dispersion compensation," *IEEE Photon. Technol. Lett.* **16**, 1516–1518 (2004).
17. F. Gérôme, J.-L. Auguste, and J.-M. Blondy, "Design of dispersion-compensating fibers based on a dual-concentric-core photonic crystal fiber," *Opt. Lett.* **29**, 2725–2727 (2004).
18. A. Huttunen and P. Törmä, "Optimization of dual-core and microstructure fiber geometries for dispersion compensation and large mode area," *Opt. Express* **13**, 627–635 (2005), <http://www.opticsinfobase.org/abstract.cfm?URI=oe-13-2-627>.
19. S. Yang, Y. Zhang, X. Peng, Y. Lu, A. Xie, J. Li, W. Chen, Z. Jiang, J. Peng, and H. Li, "Theoretical study and experimental fabrication of high negative dispersion photonic crystal fiber with large area mode field," *Opt. Express* **14**, 3015–3023 (2006), <http://www.opticsinfobase.org/abstract.cfm?URI=oe-14-7-3015>.
20. S. Kim, C. S. Kee, D. K. Ko, J. Lee, and K. Oh, "A dual-concentric-core photonic crystal fiber for broadband dispersion compensation," *J. Korean Phys. Soc.* **49**, 1434–1437 (2006).
21. P. Domachuk, H. C. Nguyen, B. J. Eggleton, M. Straub, and M. Gu, "Microfluidic tunable photonic band-gap device," *Appl. Phys. Lett.* **84**, 1838–1840 (2004).
22. J. B. Jensen, L. H. Pedersen, P. E. Hoiby, L. B. Nielsen, T. P. Hansen, J. R. Folkenberg, J. Riishede, D. Noordegraaf, K. Nielsen, A. Carlsen, and A. Bjarklev, "Photonic crystal fiber based evanescent-wave sensor for detection of biomolecules in aqueous solutions," *Opt. Lett.* **29**, 1974–1976 (2004).
23. R. Zhang, J. Teipel, and H. Giessen, "Theoretical design of a liquid-core photonic crystal fiber for supercontinuum generation," *Opt. Express* **14**, 6800–6812 (2006), <http://www.opticsinfobase.org/abstract.cfm?URI=oe-14-15-6800>.
24. L. Xiao, W. Jin, M. Demokan, H. Ho, Y. Hoo, and C. Zhao, "Fabrication of selective injection microstructured optical fibers with a conventional fusion splicer," *Opt. Express* **13**, 9014–9022 (2005), <http://www.opticsinfobase.org/abstract.cfm?URI=oe-13-22-9014>.
25. Y. Huang, Y. Xu, and A. Yariv, "Fabrication of function microstructured optical fibers through a selective-filling technique," *Appl. Phys. Lett.* **85**, 5182–5184 (2005).
26. M. Sasaki, T. Ando, S. Nogawa, and K. Hane, "Direct Photolithography on Optical Fiber End," *Jpn. J. Appl. Phys.* **41**, 4350–4355 (2002).
27. C. P. Yu and H. C. Chang, "Yee-mesh-based finite difference eigenmode solver with PML absorbing boundary conditions for optical waveguides and photonic crystal fibers," *Opt. Express* **12**, 6165–6177 (2004), <http://www.opticsinfobase.org/abstract.cfm?URI=oe-12-25-6165>.
28. Z. Zhu and T. Brown, "Full-vectorial finite-difference analysis of microstructured optical fibers," *Opt. Express* **10**, 853–864 (2002), <http://www.opticsinfobase.org/abstract.cfm?URI=oe-10-17-853>.
29. S. Guo, F. Wu, S. Albin, H. Tai, and R. Rogowski, "Loss and dispersion analysis of microstructured fibers by finite-difference method," *Opt. Express* **12**, 3341–3352 (2004), <http://www.opticsinfobase.org/abstract.cfm?URI=oe-12-15-3341>.
30. P. J. Chiang, C. P. Yu, and H. C. Chang, "Robust calculation of chromatic dispersion coefficients of optical fibers from numerically determined effective indices using Chebyshev-Lagrange interpolation polynomials," *IEEE J. Lightwave Technol.* **24**, 4411–4416 (2006).
31. W. Wadsworth, A. Witkowska, S. Leon-Saval, and T. Birks, "Hole inflation and tapering of stock photonic crystal fibres," *Opt. Express* **13**, 6541–6549 (2005), <http://www.opticsinfobase.org/abstract.cfm?URI=oe-13-17-6541>.
32. L. M. Xiao, W. Jin, M. S. Demokan, H. L. Ho, H. Y. Tam, J. Ju, and J. Yu, "Photopolymer microtips for efficient light coupling between single-mode fibers and photonic crystal fibers," *Opt. Lett.* **30**, 1791–1793 (2006).

1. Introduction

Chromatic dispersion in single-mode optical fibers causes broadening of optical pulses and has drawn a limitation on the high-speed data transmission rate in broadband wavelength division multiplexing (WDM) systems. It is required to employ dispersion compensating components for the considerable positive dispersion of installed optical fibers in the long distance optical communication systems. In order to reduce the additional losses, the dispersion compensating components should be as short as possible with a large magnitude of the negative dispersion value at the transmission wavelength. Several techniques have been proposed to compensate the effect of chromatic dispersion, including chirped fiber Bragg gratings [1,2], dispersion compensating filters [3], high-order mode fibers [4,5], and the most widely used dispersion compensating fibers (DCFs) [6–9]. These DCFs contain two spatially separated asymmetric concentric cores which support two supermodes: inner mode and outer mode. By an appropriate design, mode matching of these two supermodes can be achieved at a specified wavelength λ_p with a high negative dispersion coefficient D . DCFs have been

theoretically investigated to provide $-5100\text{-ps}/(\text{nm}\cdot\text{km})$ dispersion compensation [6] and experimentally shown to have a dispersion value of $-1800\text{ ps}/(\text{nm}\cdot\text{km})$ at the wavelength $\lambda = 1.55\ \mu\text{m}$ [7].

Except for DCFs, photonic crystal fibers (PCFs) with periodic air holes along its entire length have also been demonstrated to possess the ability of dispersion tailoring [10,11] and the potential to function as useful dispersion compensating devices [12–15]. By adjusting the geometric parameters of PCFs, including the lattice constants and the sizes of air holes, high negative dispersion values over a wide wavelength range can be achieved. Similar to the basic design of DCFs, an outer ring with larger refractive index than that of the photonic crystal cladding is introduced in the PCF structure to form a dual-core PCF [16–20]. The inner core is fabricated by a missing air hole in a two-dimensional triangular photonic crystal cladding and the larger index of the outer ring can be accomplished by replacing the original air holes with smaller ones or just by filling up these holes with silica. Prior theoretical investigation [17] has achieved $-2200\text{-ps}/(\text{nm}\cdot\text{km})$ dispersion value at $\lambda = 1.55\ \mu\text{m}$ with lattice constant $\Lambda = 2.3\ \mu\text{m}$, air-hole diameter $d = 1.4\ \mu\text{m}$, and a smaller air-hole diameter $\phi = 0.51\ \mu\text{m}$ in the outer ring. The value of the dispersion coefficient D and the phase-matching wavelength λ_p can be tuned by adjusting the air-hole diameters and the lattice constants. But it is hard to fabricate such smaller air holes in the outer ring with a specified hole diameter.

To obtain a larger magnitude of the negative dispersion value, a doped inner core was introduced in the dual-core PCF structures [18,19]. The dispersion value can be highly improved to be $-55000\text{ ps}/(\text{nm}\cdot\text{km})$ [18] which is better than other similar structures. However, a highly doped core will lead to possible occurrence of higher order modes which may interfere with the fundamental mode. Besides, a MCVD process is needed to realize such a high-index core in the fabrication [19].

Instead of decreasing air-hole sizes, one can also insert liquid in the cladding region to form an outer core. Several techniques have been proposed for selectively filling the air holes in PCFs with liquid for useful applications, such as tunable optical filters [21], sensors [22], and supercontinuum generation [23]. By utilizing the fusion splicing technique with tailored electric arc energies and fusion times, one can selectively fuse the cladding region of the PCF [24]. Through different flow speeds of the liquid in air holes of various sizes, one can selectively fill liquid in the air core or air cladding in hollow PCFs [25]. To make it more precisely, the photo-lithographic masking technique [26] can be adopted to block unwanted air holes at the end-face of PCFs to achieve the selective filling.

For these improvements in selectively filling air holes with liquid in PCF structures, we propose another design for DCFs based on dual-core PCFs with the fourth layer of air holes filled with high-index liquid. A full-vector finite-difference frequency-domain (FDFD) method [27] will be adopted to find out the effective indices of the guided modes as well as the corresponding dispersion values. By varying the air-hole diameters and liquid indices, the dispersion characteristics of the proposed DCF structures will be investigated. We also analyze the temperature dependence of the dual-core liquid-filled PCFs to design a tunable dispersion compensating device for optical communication systems.

2. Geometry and the numerical methods

The outer core of the dual-core PCF can be fabricated by selectively filling air holes with liquid in the cladding region. In addition to the mentioned selectively filling techniques [24–26], the dual-core liquid-filled PCF can also be fabricated by the following steps. Start with a fiber preform composed of silica capillaries and a silica rod at the center. Using a drawing tower, we can have a microstructured PCF connected with the microscopic preform as demonstrated in Fig. 1(a). It is relatively approachable to precisely insert the liquid into the microscopic fiber preform than into the microstructured PCF. Thus, we can simply pour the liquid into the selected capillaries in the preform and drift it to the PCF through the connected air channel by an applied pressure.

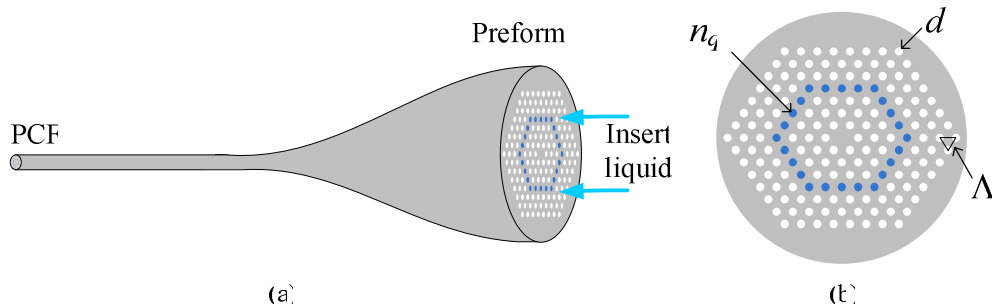


Fig. 1. (a) Illustration of possible fabrication for selectively inserting liquid into the PCF through the fiber preform. (b) Cross-sectional view of the dual-core liquid-filled PCF for dispersion compensation.

Figure 1(b) is the cross-sectional view of the dual-core liquid-filled PCF. The liquid with the refractive index larger than air raises the effective index of the fourth layer which functions as the outer core in the dual-core PCF. In this design, the refractive index and the shape of the inner core remain unchanged as the original PCF to keep the single-mode operation in the inner-core region. The full-vector FDFD method which is an efficient and accurate numerical mode solver for the analysis of optical waveguides and PCFs [27–29] is utilized to obtain the propagation characteristics of the dual-core liquid-filled PCF. For the symmetric geometry, only one quarter of the PCF is taken into account with perfectly matched layers (PMLs) as the absorbing boundary conditions. After finding out the effective indices n_{eff} 's of the fundamental guided modes on the PCF at various wavelengths, the dispersion values D can then be deduced according to

$$D = \frac{-\lambda}{c} \frac{d^2 n_{eff}}{d\lambda^2} \quad (1)$$

where c is the speed of light in vacuum. To improve numerical accuracy, the proper boundary condition matching scheme is adopted in our FDFD mode solver to deal with the dielectric discontinuities in the PCF structure [27].

3. Dispersion characteristics

We first consider the DCF based on the dual-core liquid-filled PCF shown in Fig. 1(b) with $\Lambda = 2.3 \mu\text{m}$, $d = 1.2 \mu\text{m}$, and the refractive index of the liquid n_q being 1.3875. The fourth layer of air holes is filled with liquid to form the outer core in the PCF with phase-matching wavelength λ_p around $1.55 \mu\text{m}$ for optical communications. By utilizing the FDFD mode solver, we can obtain the modal effective indices n_{eff} 's of the guided modes on the PCF structure, shown in Fig. 2(a), as well as the field distributions of the fundamental mode at variant wavelengths, displayed in Fig. 3. In Fig. 2(a), the solid and dashed lines represent effective index curves for the fundamental and second-order modes, respectively. For $\lambda < 1.55 \mu\text{m}$, the inner mode is the fundamental mode with the transmitted power well confined in the central region as shown in Fig. 3(a) for $\lambda = 1.52 \mu\text{m}$. Around $\lambda = 1.55 \mu\text{m}$, the n_{eff} 's of these two modes are so close as optical coupling between them can be induced. In Fig. 3(b), we can see that the light field starts to spread out from the inner core to the outer core and a rapid change in the slope of the effective index curve can be observed in Fig. 2(a). For $\lambda > 1.55 \mu\text{m}$, most power spreads from the inner core to the outer core and is well confined in the outer core region as illustrated in Fig. 3(c) for $\lambda = 1.58 \mu\text{m}$. Thus, the outer mode possesses larger n_{eff} than the inner mode as shown in Fig. 2(a). The corresponding losses of the guided modes versus the wavelength are demonstrated in Fig. 2(b). One can see that both the fundamental (solid line) and second-order (dashed line) modes possess small propagation losses. Besides,

the loss of the fundamental mode rises sharply around the phase-matching wavelength and increases slowly as the outer mode being the fundamental mode as shown in Fig. 2(b).

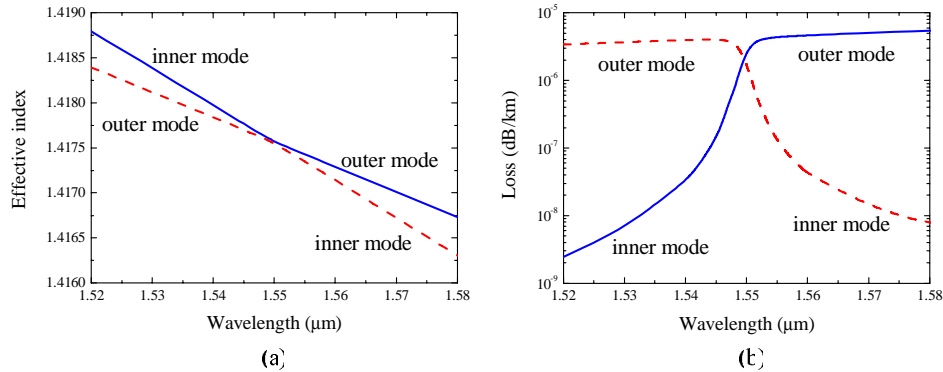


Fig. 2. (a) Effective indices and (b) losses versus the wavelength for the fundamental (solid line) and second-order (dashed line) modes.

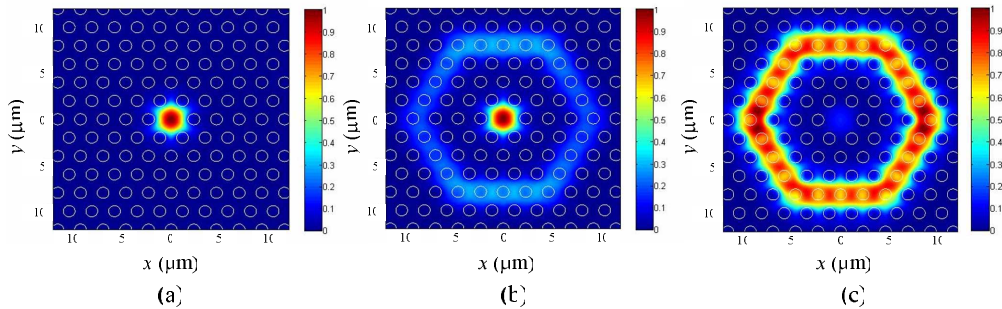


Fig. 3. Field distributions for the fundamental modes on the dual-core liquid-filled PCF for $\lambda =$ (a) 1.52 μm , (b) 1.55 μm , and (c) 1.58 μm , respectively.

We can then obtain the values of the dispersion D deduced according to Eq. (1) for the fundamental and second-order modes of the dual-core liquid-filled PCF by an efficient scheme using Chebyshev-Lagrange interpolation polynomials [30]. The two curves show highly symmetric properties owing to the coupling between the two modes as seen in Fig. 4. Due to the rapid slope changes of the modal index curves caused by the mode coupling, very large values of D appear around λ_p for both the fundamental and second-order modes. By a proper design, the value of D for the fundamental mode can reach -19000 ps/(nm·km) at $\lambda = 1.55$ μm . The very high negative D value can help us decrease the length of the DCF structures and reduce possible losses. Moreover, the negative dispersion slope for $\lambda < \lambda_p$ could also be useful for some applications in WDM systems.

Figure 5(a) shows the effective index curves of the same PCF with the liquid filled in variant air-hole layers and the corresponding dispersion values are displayed in Fig. 5(b). As we increase the number of air-hole layers between the inner and outer cores, the appearance of rapid slope changes in the index curves due to the optical coupling moves toward larger wavelength. The solid and dashed lines in the inset of Fig. 5(a) represent the calculated index curves for the original PCF without liquid and PCFs with only an outer core containing liquid, respectively. One can observe that the effective index decreases as we move the liquid-core ring outward, leading to the phase-matching wavelength shifting to the larger wavelength. Besides, larger distance between the inner and outer cores will also suppress the occurrence of optical coupling between two cores, resulting in more incisive tips on the index curves and

narrower full-width at half-maximum (FWHM) with a highly increasing dispersion value as shown in Fig. 5(b). Although $D = -28000$ ps/(nm-km) can be achieved with liquid filled in the fifth layer, we will focus on the dispersion properties of dual-core PCFs with the fourth air-hole layer filled with liquid in the following discussion.

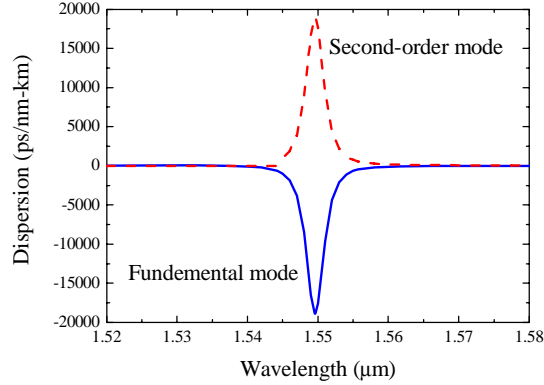


Fig. 4. Dispersion values versus the wavelength for the fundamental and second-order modes.

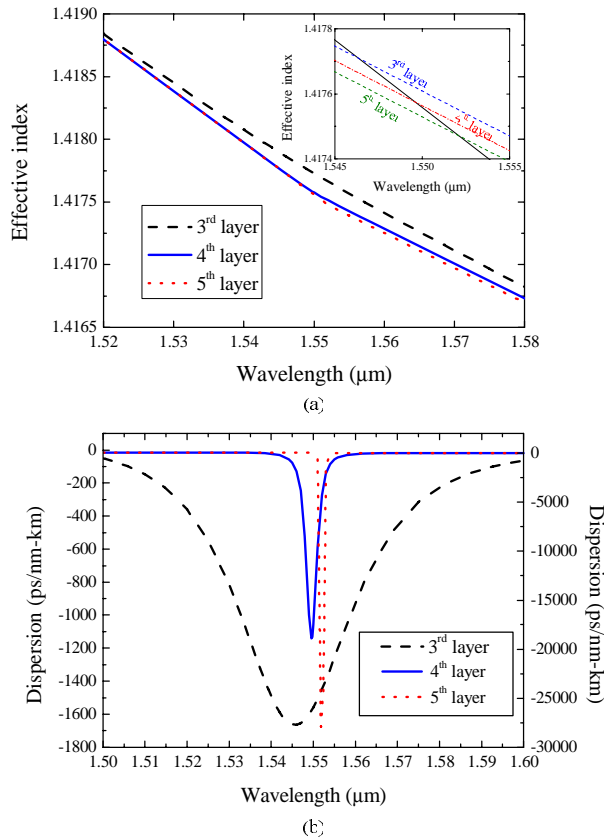


Fig. 5. (a) Effective index curves for the dual-core PCF in Fig. 1(b) with the liquid filled in variant air-hole layers. (b) Dispersion values of the dual-core PCF with the liquid filled in variant air-hole layers.

Figure 6 demonstrates the dispersion values of dual-core liquid-filled PCFs with the air-hole diameter being 1.1 μm , 1.2 μm , and 1.3 μm , respectively. Unlike the variation of the liquid filled in variant air-hole layers, the change in the air-hole diameter dramatically moves the position of λ_p due to the different matching claddings. Similar to the liquid filled in outer air-hole layers, larger air-hole possesses relatively large negative D values and sharper deeps at longer λ_p as shown in Fig. 6. For example, $D = -48000$ ps/(nm-km) can be achieved for $d = 1.3$ μm at $\lambda = 1.645$ μm . By appropriately designing the geometry of the PCF, we can realize a DCF with a very large negative dispersion at the desired wavelength for optical communications.

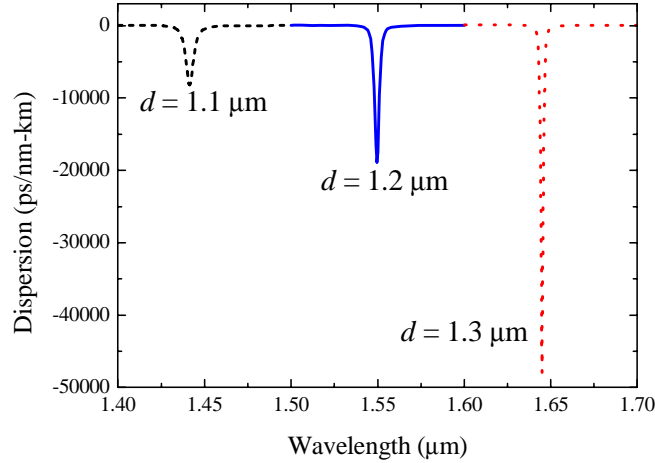


Fig. 6. Dispersion values of dual-core liquid-filled PCFs with variant air-hole sizes.

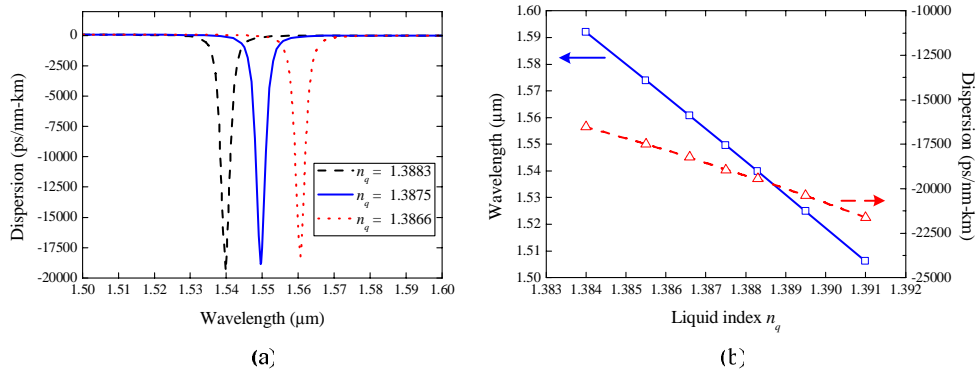


Fig. 7. (a) Dispersion curves for dual-core liquid-filled PCF in Fig. 1(b) with various liquid indices n_q . (b) Corresponding phase-matching wavelengths and dispersion values for various liquid indices n_q .

4. Tunability properties of dual-core liquid-filled PCFs

Although PCFs possess the attractive properties of tailoring dispersion by geometric parameters, the dispersion characteristics of a PCF is fixed once it is fabricated. To obtain an optimal or a slightly different design, one should produce a newer one with different geometry. Thanks to the liquid-filled outer core, we can introduce tunable dispersion properties in our

dual-core PCFs by choosing liquid with various refractive indices. Figure 7(a) shows the dispersion D of the DCF in Fig. 1(b) with n_q being 1.3866, 1.3875, and 1.3883, respectively. One can see that the liquid index changes the position of the phase-matching wavelength as well as the value of dispersion. We further vary the liquid index n_q from $n_q = 1.384$ to $n_q = 1.391$ and calculate the corresponding phase-matching wavelengths λ_p and the largest values of D . Both the values of λ_p and D display linear-like dependence on the liquid index as shown in Fig. 7(b). With increasing n_q , the effective index of the outer core mode is raised, which moves λ_p to shorter wavelengths. Meanwhile, the values of D remains larger than -16000 ps/(nm-km) as we change the liquid index. Thus, we can easily tune the position of λ_p to our desired value by inserting the outer core with liquid having various refractive indices.

To demonstrate the tunability of the dual-core liquid-filled PCF for dispersion compensation, we choose the filling liquid from Cargille Laboratories with n_q close to 1.3875 at 25°C. The thermo-optic coefficient of the liquid is $-3.45 \times 10^{-4} \text{ } ^\circ\text{C}^{-1}$ which is much larger than that of the fused silica. By controlling the operation temperature, the value of n_q can be varied and the phase-matching wavelength λ_p can be well tuned. Figure 8(a) shows the calculated dispersion curves for the dual-core liquid-filled PCF operated at 17.5°C, 25°C, and 32.5°C, respectively. In our simulations, the material dispersions of silica and filling liquid are also taken into account, which should have less effect than the waveguide dispersion. It can be seen that the phase-matching wavelength moves to larger wavelength with the raise of the temperature. We also calculate the values of λ_p for various temperatures as shown in Fig. 8(b) and a linear relationship between λ_p and the temperature can be observed with the positive slope 4.31 nm/°C.

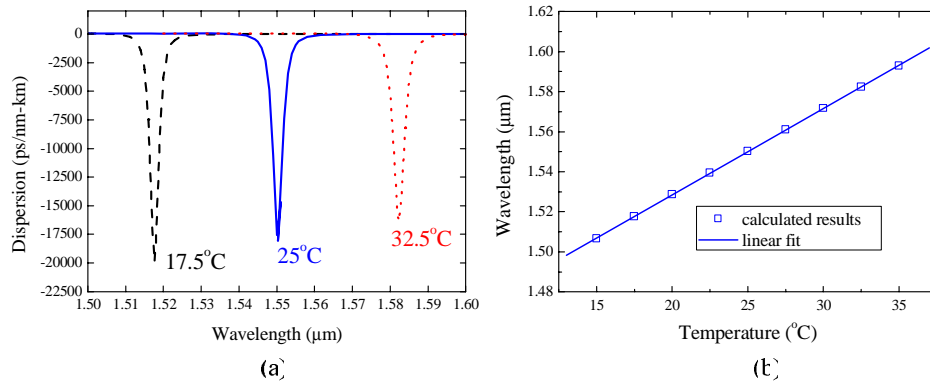


Fig. 8. (a) Dispersion curves for a dual-core liquid-filled PCF operated at variant temperatures. (b) Phase-matching wavelengths for a dual-core liquid-filled PCF operated at variant temperatures.

By considering the material loss of the filling liquid provided by Cargille Laboratories, the calculated propagation loss of the dual-core liquid-filled PCF is 2.86 dB/km at $\lambda = 1.55 \text{ } \mu\text{m}$. Since our proposed structure possesses a very high negative chromatic dispersion value D , the length of the device can be efficiently reduced as well as the total propagation loss. For example, for a 20-km SMF-28 we only need a 18-m dual-core liquid-filled PCF to perform the required dispersion compensation and the propagation loss is 0.05 dB. This kind of device also has the potential to be employed in other optical applications which only require a short device length. However, the theoretical coupling loss of our proposed structure to the SMF-28 is 4.22 dB. This high value is mainly due to the mismatch of the mode field diameters (MFDs) of these two waveguides. To reduce the coupling loss, we can adopt another PCF having similar MFD with that of the SMF-28 or use tapered PCFs [31] or microtips [32] to increase the coupling between the small PCF and the SMF-28.

From these calculated results, one can see that our proposed dual-core liquid-filled PCFs not only function as useful tunable dispersion compensating devices for optical communication but also can help to correct possible fabrication errors in the geometry of PCF structures. Even we have mismatch in the produced PCF structures with the optimal design by simulation, the phase-matching wavelength can still be tuned to our desired value by varying the liquid index with operation temperature, which does help a lot for the development of DCF structures.

5. Conclusions

We have proposed a dispersion compensating structure based on the dual-core liquid-filled PCF with one of the outer rings filled with liquid. Applying the full-vector FDFD mode solver, we can obtain the effective indices and the field distributions of the guided modes on the proposed structures. By varying the layer of the liquid-core and the sizes of air holes, we have investigated the dispersion characteristics of the dual-core PCFs. A very high negative chromatic dispersion value $D = -19000$ ps/(nm-km) can be achieved at $\lambda = 1.55$ μm and the phase-matching wavelength can also be tuned by the geometry of the PCF. We also demonstrate the tunability properties of the proposed devices. The phase-matching wavelength can be well tuned by the liquid index which can be controlled by the operation temperature. The tunability of the dual-core liquid-filled PCF can be utilized to work in wide wavelength range and can help correct possible fabrication mismatches in the geometry of PCF structures.

Acknowledgments

This work was supported by the National Science Council of the Republic of China under Grants No. NSC95-2811-E-002-043 and No. NSC96-2218-E-110-009 and by the Ministry of Education of the Republic of China under an "Aim for the Top University Plan" grant.